PHARMACOLOGY 2019

15–17 December | Edinburgh

SUBMIT AN ABSTRACT

- Participate in the UK's leading pharmacology event

- Share your research with over 1,200 attendees

- Apply for awards and attendance bursaries

- Have your work published in the British Journal of Pharmacology or the British Journal of Clinical Pharmacology

SUBMIT NOW

Deadline to submit

9 September

BRITISH PHARMACOLOGICAL SOCIETY

@BritPharmSoc #Pharmacology2019

Ianaro Angela (Orcid ID: 0000-0003-3954-4083)

TITLE

Modulation of myeloid derived suppressor cells (MDSCs) functions: a new strategy towards hydrogen sulfide anti-cancer effects

RUNNING (SHORT) TITLE

H_2S is a novel MDSCs regulator

AUTHOR INFORMATION

Paola De Cicco[1], Giuseppe Ercolano[1], Valentina Rubino[2,3], Giuseppe Terrazzano[2,3], Giuseppina Ruggiero[2], Giuseppe Cirino[1], Angela Ianaro*[1].

[1] *Department of Pharmacy, University of Naples Federico II, Naples, Italy*
[2] *Department of Translational Medical Sciences, University of Naples Federico II, Naples, Italy*
[3] *Department of Science, University of Basilicata, Potenza, Italy*

Corresponding author
Angela Ianaro*[1].

Word count: 3131

Conflict of interest

The authors declare no conflicts of interest.

ABSTRACT

Background and Purpose: Myeloid-derived suppressor cells (MDSCs) represent the major obstacle to cancer treatment. In fact, MDSCs negatively regulate antitumor immunity through the suppression of tumor-specific T lymphocytes. Thus, the efficacy of immunotherapies may be improved by targeting MDSCs. In this study, we investigated on the ability of hydrogen sulfide (H_2S), a gasotransmitter whose anti-cancer effects are well-known, to inhibit MDSCs accumulation and immunosuppressive functions in melanoma.

Experimental Approach: The effect of H_2S on the host immune response to cancer was evaluated using an *in vivo* syngeneic model of murine melanoma. B16F10-melanoma-bearing mice were treated with diallyl trisulfide (DATS) and analyzed for immune cells composition in relation to MDSCs, dendritic cells (DCs) and T-cells. Moreover, we evaluated H_2S effect on MDSCs immunosuppressive genes expression and on T-cell proliferation.

Key Results: In melanoma-bearing mice, DATS inhibited tumor growth and this effect was associated with a reduction in the frequency of MDSCs in the spleen, in the blood as well as in the tumor microenvironment. In addition, we found that CD8$^+$ T cells and DCs were increased. Furthermore, DATS reduced MDSCs immune suppressive activity restoring T cells proliferation.

Conclusion and Implications: This study demonstrate that DATS inhibits the expansion and the suppressive functions of MDSCs, suggesting a novel role for H_2S in the modulation of MDSCs in cancer. Therefore, H_2S-donors may provide a novel approach for enhancing the efficacy of melanoma immunotherapy.

Key words: hydrogen sulfide, melanoma, MDSC, immunity, T cell, immunotherapy.

NON-APPROVED ABBREVIATIONS

Arginase 1 (ARG1)

Cystathionine-β synthase (CBS)

Cystathionine-γ lyase (CSE)

Diallyl Trisulfide (DATS)

Hydrogen sulfide (H_2S)

Inducible nitric oxide synthase (iNOS)

L-arginine (L-Arg)

L-cysteine (L-Cys)

Myeloid-derived suppressor cells (MDSCs)

3-mercaptopyruvate sulfurtransferase (3-MST)

Bullet point summary

<u>What is already known</u>

- MDSCs are responsible for immunotherapy resistance in melanoma patients
- H_2S donors can suppress cancer cells proliferation via various mechanisms

<u>What this study adds</u>

- To investigate on the ability of H_2S to shape the host immune response to cancer

<u>Clinical significance</u>

- To provide a new therapeutic strategy to inhibit MDSCs differentiation and function
- To develop new H_2S-based drugs for enhancing the efficacy of T cell-mediated melanoma immunotherapy.

List of Hyperlinks

<u>nitric oxide</u> (<u>NO</u>)

<u>L-arginine</u> (<u>L-Arg</u>)

<u>Arginase 1</u> (<u>ARG1</u>)

<u>inducible nitric oxide synthase</u> (<u>iNOS</u>)

<u>L-cysteine</u> (<u>L-Cys</u>)

<u>hydrogen sulfide</u> (<u>H_2S</u>)

<u>cystathionine-β synthase</u> (<u>CBS</u>)

<u>cystathionine-γ lyase</u> (<u>CSE</u>)

<u>3-mercaptopyruvate sulfurtransferase</u> (<u>3-MST</u>)

<u>GM-CSF</u>

<u>IL-4</u>

<u>IL-10</u>

<u>heme oxygenase-1</u> (<u>HMOX-1</u>)

<u>TGFβ</u>

<u>COX2</u>

<u>indoleamine 2,3-dioxygenase</u> (<u>IDO</u>)

<u>GSH</u>

Introduction

Aberrant differentiation of myeloid cells is one of the hallmarks of cancer. Expansion and accumulation of dysregulated and functionally impaired immune cells in the tumor microenvironment lead to cancer progression and failure of immunotherapeutic attempts (Kerkar *et al.*, 2012). Myeloid-derived suppressor cells (MDSCs) represent the major components of this immune-suppressive network responsible for cancer-associated immune evasion. Above all else, MDSCs are directly implicated in the promotion of tumour cell survival, angiogenesis, tumour cell invasion and metastases (Condamine *et al.*, 2015). MDSCs are a heterogeneous population of immature myeloid cells with potent immune suppressive activity based on inhibition of tumor-specific CD8$^+$ cytotoxic T lymphocytes. The main immunosuppressive mechanism driven by MSDCs involves the nitric oxide (NO) pathway. In particular, a key role for L-arginine (L-Arg) metabolism, shifted toward Arginase 1 (ARG1) and inducible nitric oxide synthase (iNOS) has been demonstrated in these cells (Gabrilovich *et al.*, 2009). Thus, a decreased availability of L-Arg combined with the accumulation of NO derivatives (NO_2^-, NO_3^-, N_2O_3) triggers the inhibition of T-cell function and proliferation (Bronte *et al.*, 2003). The non-essential aminoacid L-cysteine (L-Cys) is recently gaining attention in the modulation of the immune response. Indeed, L-Cys is required for protein synthesis and cell proliferation as well as for antigen presentation and subsequent T-cell activation (Yan *et al.*, 2010). Furthermore, both L-Cys and L-Arg are the precursor of two important gasotransmitters: hydrogen sulfide (H_2S) and NO, respectively. The former is produced in various mammalian cells and tissues by three principal enzymes: cystathionine-β synthase (CBS), cystathionine-γ lyase (CSE) and 3-mercaptopyruvate sulfurtransferase (3-MST). H_2S is an endogenous signaling molecule with a plethora of cellular and molecular targets (Wallace *et al.*, 2015). One of the most extensively investigated mechanism of H_2S is its antioxidant effects. It acts as dominant redox regulator of several aspects of physiological and pathophysiological functions (Stein *et al.*, 2013). Thus, changing the redox status of the environment could impair T cell activity. In particular, we hypothesize that MDCSs in their effector state deprive the indispensable H_2S to support T cell activation and function.

Therefore, we used an *in vivo* syngeneic model of murine melanoma to investigate on the ability of H_2S to shape the host immune response to cancer. Recently, frequency of suppressive MDSCs has been associated with progression and recurrence in melanoma patients (Jordan *et al.*, 2013). Since immunotherapy is the most promising systemic therapy

for patients with advanced melanoma, the development of new drugs targeting MDSCs may represent a useful strategy to solve this unmet need. Naturally occurring H_2S donors, such as diallyl trisulfide (DATS) and acetyl deacylasadisulfide, have been demonstrated to induce apoptosis in human melanoma cells and to inhibit metastatic melanoma development and progression (Panza *et al.*, 2015; De Cicco *et al.*, 2017). In this study, we confirmed the antitumor effect of DATS and investigated on the ability of the H_2S-donor to modify the immune cells profile in tumor microenvironment focusing on MDSCs. The results show that oral administration of DATS in melanoma-bearing mice decrease MDSCs number in the tumour microenvironment and in peripherals lymphoid organs as well as abrogate their immunosuppressive activity. In addition, increasing H_2S level helps to restore an anti-tumour immune response promoting T cell proliferation, which results in a remarkable inhibition of tumour growth. Therefore, H_2S-donors may provide a new therapeutic strategy for enhancing the efficacy of T cell-mediated melanoma immunotherapy.

Methods

Animals

Female C57BL/6J mice, 6- weeks- old and weighing 18–20 g, were purchased from Charles River Laboratories (Germany). The experimental procedures were approved by the Italian Ministry in accordance with Italian (DL 26/2014) and European (Directive 2010/63/EU) regulations on the protection of animals used for experimental and other scientific purposes. Animal studies are reported in compliance with the ARRIVE guidelines (Kilkenny *et al.*, 2010; McGrath *et al.*, 2015).All the animals were housed at the Animal Research Facility of the Department of Pharmacy of the University of Naples Federico II. They were subdivided in groups of five animals in clear- transparent plastic cages with autoclaved dust- free sawdust bedding. They were fed a pelleted and had unrestricted access to food and drinking water. The light/dark cycle in the room consisted of 12/12 h with artificial light. Mice were killed by CO_2 inhalation.

Cell lines and media

The murine melanoma cell line B16F10 (ICLC Cat# ATL99010, RRID:CVCL_0159) was purchased from IRCCS AOU San Martino – IST (Genova, Italy) and was cultured in DMEM containing 10% FBS, 2 mmol/L L-glutamine, 100 µmol/L non essential amino acids, penicillin (100 U/mL), streptomycin (100 µg/mL) and 1 mmol/L sodium pyruvate (all from Sigma-Aldrich, Milan, Italy). Cells were grown at 37°C in a humidified incubator under 5% CO2.

Induction of subcutaneous melanoma

The B16F10 syngeneic murine melanoma model has been widely used to study the mechanisms of melanoma development and progression and to evaluate the effect of any candidate drug (McKinney *et al.*, 2011). B16F10 murine melanoma cells (1×10^5) in 100 μL saline were injected s.c. into the right flank of C57BL/6 mice (7 weeks-old). Animals were randomly divided into two groups of 8 animals each: one control group and one treatment group. The control group was treated with vehicle (0.5% carboxymethyl cellulose/0.1% DMSO in double distilled water) whereas the other group received DATS (50mg/Kg), as previously described (Panza *et al.*, 2015). Vehicle or DATS were administered by oral gavage every day. Treatments were started immediately after the injection of the tumour cells and continued until day 21. All efforts were made to minimize suffering. Mice were observed daily and humanely euthanized by CO_2 inhalation if a solitary subcutaneous tumor exceeded 1.5 cm in diameter or mice showed signs referable to metastatic cancer. Tumor sizes were measured using a digital caliper and tumor volumes were calculated using the following equation: tumor volume=$\pi/6$(D1xD2xD3) where D1=length; D2=width; D3= height and expressed as cm^3. Drug preparation, treatment, and animal data collection were conducted blindly and independently by two investigators.

Preparation of a single cell suspension from spleen, tumour and peripheral blood of melanoma-bearing mice

Spleens were harvested and disrupted mechanically to prepare single cell suspensions, which were then incubated in red blood cell (RBC) lysis buffer (Biolegend, San Diego, CA) for 5 minutes at room temperature. Single-cell suspensions from tumor tissue were prepared using the GentleMACS single cell isolation protocol (Miltenyi Biotec, Bergisch Gladbach, Germany). Briefly, tumors were isolated and minced into small pieces followed by a mechanical dissociation step using the GentleMACS dissociator (Miltenyi Biotec, Bergisch Gladbach, Germany). Samples were then incubated for 40 min at 37°C with the following enzymes: collagenase I (10,000 U/ml) and dispase II (32 mg/ml). After the last mechanical disruption step, the digested tumors were harvested, filtered (over a 70 μM nylon filter) and red blood cells were lysed by adding RBC buffer. Whole blood was collected in heparinized tubes by cardiac puncture and leukocytes were isolated by using erythrocyte sedimentation followed by 2 rounds of lysis with RBC buffer. The resulting cells from spleen, tumor and blood were resuspended in PBS with 1% BSA and counted with a haemocytometer and Trypan blue.

Flow cytometry

Aliquots of 5 x 10^5 cells were incubated with anti-Fc receptor (αCD16/32) (Thermo Fisher Scientific Cat# 14-0161, RRID:AB_467135) and then stained using the following panel of monoclonal antibodies (mAbs) to murine cell surface molecules (all from eBiosciences Inc. San Diego, CA): PerCP-Cy5.5-conjugated anti-CD11b (Thermo Fisher Scientific Cat# 45-0112-82, RRID:AB_953558), PE-conjugated anti-Ly6G (Thermo Fisher Scientific Cat# 12-9668-80, RRID:AB_2572719), Alexa Fluor 488-conjugated anti-Ly6C (Thermo Fisher Scientific Cat# 53-5932-80, RRID:AB_2574426), APC-coniugated anti-CD45 (Thermo Fisher Scientific Cat# 17-0451, RRID:AB_469393), Alexa Fluor 488-conjugated anti-CD11c (Thermo Fisher Scientific Cat# 53-0114, RRID:AB_469902), APC-coniugated anti-F4/80 (Thermo Fisher Scientific Cat# 17-4801, RRID:AB_469452), FITC-conjugated anti-CD3 (Thermo Fisher Scientific Cat# 11-0031, RRID:AB_464881), PerCP-Cy5.5-conjugated anti-CD8 (Thermo Fisher Scientific Cat# 45-0081-82, RRID:AB_1107004). Flow cytometry and data analysis were performed by using a two-laser equipped FACSCalibur apparatus and the CellQuest analysis software (Becton Dickinson, Mountain View, CA).

Proliferation assay

Splenocytes from healthy C57BL6 mice, depleted of red cells, were placed in triplicates into U-bottom 96-well plates (3×10^5/well) and stimulated with coated 3 µg/ml anti-CD3 (BioLegend Cat# 100238, RRID:AB_2561487) antibody and 2 µg/ml anti-CD28 antibody (BioLegend Cat# 102112, RRID:AB_312877). MDSCs were purified from the spleen of C57BL6 melanoma-bearing mice using mouse MDSC isolation kits (Miltenyi Biotec, Bergisch Gladbach, Germany) according to the manufacturer's protocol and then added to splenocytes ad different ratio. Cells were cultured in a humidified 5% CO_2 atmosphere at 37°C for 72 h, and [^{3}H]-thymidine (1 µCi/well; Promega) was added 18h before harvesting. ^{3}H-thymidine uptake was counted using a scintillation counter (Beckman Coulter, Brea, CA, USA) and expressed as counts per minute (CPM).

Fluorescence measurement of H$_2$S

The fluorescent dye WSP-1 (Cayman Chemical, Ann Arbor, MI,USA) was used to assess H_2S levels in the plasma of C57BL/6 melanoma-bearing mice or in the supernatant of BM-MDSCs. WSP-1 (100 µM) fluorescence was determined (Ex$_{465nm}$, Em$_{515nm}$) using GloMax®-Multi Detection System microplate reader (Promega, Milan, Italy) at 30 min.

Western Blot Analysis

Whole-cell extracts were prepared from melanoma tissue homogenate, as previously described (Panza *et al.*, 2015). The protein concentration was measured by the Bradford

method (Bio-Rad, Milan, Italy). Equal amounts of protein (50 µg/sample) were separated by SDS-PAGE and blotted onto nitrocellulose membranes (Trans-Blot Turbo Transfer Starter System, Biorad). The membranes were blocked for 2 hours in 5% low-fat milk in PBS with 0.1% Tween 20 (PBST) at room temperature. Then the filters were incubated with the following primary antibodies: anti-CSE (Proteintech Group Cat# 12217-1-AP, RRID:AB_2087497; diluited 1:1000), anti-CBS (Proteintech Group Cat# 14787-1-AP, RRID:AB_2070970; diluited 1:1000) and anti-β-actin (Santa Cruz Biotechnology Cat# sc-47778 HRP, RRID:AB_2714189; diluted 1:5000), overnight at 4°C. The membranes were washed 3 times with PBST and then incubated with anti-mouse (Santa Cruz Biotechnology Cat# sc-2005, RRID:AB_631736; diluted 1:2000) or anti-rabbit (Jackson ImmunoResearch Labs Cat# 111-035-144, RRID:AB_2307391; diluted 1:5000) horseradish peroxidase-conjugated antibodies for 2 h at room temperature. The immune complexes were visualized by the ECL chemiluminescence method and acquired by ChemiDoc™ MP Imaging System (Bio-Rad, Milan, Italy).

Ex vivo generation of MDSCs and flow cytometry

Bone marrow (BM) cells were obtained from femurs and tibias of C57BL/6 mice, and the red blood cells were lysed. One million cells were seeded into 6-wells plates in RPMI 1640 medium supplemented with 10% FBS, 10 ng/ml GM-CSF, 10 ng/ml IL-4 (both Miltenyi Biotec, Bergisch Gladbach, Germany), 2-ME 50 µM supplemented with 30% v/v of B16F10 cell-derived conditioning medium (CM). The cultures were maintained at 37°C in 5% CO_2-humidified atmosphere. On day 3rd of culture, floating cells were gently removed, and fresh medium with cytokines, 30% v/v of B16F10-CM with or without DATS 30µM was added. Cells were collected on day 5th and analyzed by flow cytometry. For MDSCs staining, cells were incubated with Alexa Fluor 488-conjugated anti-Ly6C, PerCP-Cy5.5- coniugated anti-CD11b and PE-coniugated anti-Ly6G antibodies for 30' at 4 °C. For dendritic cells staining, cells were incubated with Alexa Fluor 488- coniugated anti-CD11c, PerCP-Cy5.5-coniugated anti-CD11b and APC-coniugated anti-CD45 antibodies for 30' at 4 °C. For intracellular staining of ARG1 and iNOS, cells were fixed, permeabilized with Intracellular Fixation & Permeabilization Buffer (eBiosciences), washed with a 1X Permeabilization Buffer (eBiosciences) and stained with APC-coniugated anti-ARG1 (R&D System RRID:AB_2810265) and PE-Cyanine7-coniugated anti-NOS2 (Thermo Fisher Scientific Cat# 25-5920-82, RRID:AB_2573499). After washing, the samples were analyzed using BriCyte E6 (Mindray, P.R. China).

RNA purification and quantitative real-time PCR (qPCR)

Total RNA was isolated from MDSCs, purified from the spleen as above described, or from melanoma tissue, by using TRI-Reagent (Sigma-Aldrich, Milan, Italy), according to the manufacturer's instructions, followed by spectrophotometric quantization. Final preparation of RNA was considered DNA- and protein-free if the ratio between readings at 260/280 nm was ≥1.7. Isolated mRNA was reverse-transcribed by use of iScript Reverse Transcription Supermix for RTqPCR (Bio-Rad, Milan, Italy). Then, quantitative real-time-PCR was performed using CFX384 real-time PCR detection system (Bio-Rad, Milan, Italy). Primer sequences were:

ARG-1: 5'-CTGGTTGTCAGGGGAGTGTT-3'; GTGAAGAACCCACGGTCTGT-3'

iNOS: 5'-CGAAACGCTTCACTTCCAA-3'; 5'-TGAGCCTATATTGCTGTGGCT-3'

IL-10: 5'-CGGAAACAACTCCTTGGAAA-3'; 5'-AAGTGTGGCCAGCCTTAGAA-3'

HMOX-1: 5'-GCCGTGTAGATATGGTACAAGGA-3'; 5'-AAGCCGAGAATGCTGAGTTCA-3'

GCLM: 5'-AGGAGCTTCGGGACTGTATCC-3'; 5'-GGGACATGGTGCATTCCAAAA-3'

GCLC: 5'GTTGGGGTTTGTCCTCTCCC-3'; 5'-GGGGTGACGAGGTGGAGTA-3'

β-actin: 5'-TACCACCATGTACCCAGGCA-3'; 5'-CTCAGGAGGAGCAATGATCTTGA-3'

Samples were amplified in triplicate using SYBR Green master mix kit (Bio- Rad, Milan, Italy). A non-template control blank for each primer pair was used to control for contamination or primer dimers formation, and the Ct value for each experimental group was determined. The β-actin housekeeping gene was used as an internal control to normalize the Ct values, using the $2^{-\Delta Ct}$ formula.

Measurement of NO production in BM-MDSCs

Equal volumes of supernatants from BM-MDSCs culture (100 μl) were mixed with Greiss reagent (1% sulfanilamide in 5% phosphoric acid and 0.1% N-1-naphthylethylenediamine dihydrochloride in double-distilled water). After incubation at room temperature for 10 min, the absorbance at 550 nm was measured using a microplate photometer reader (Multiskan FC, Thermo Scientific™, Waltham, Massachusetts, USA). Nitrite concentrations were determined by comparing the absorbance values for the test samples with a standard curve generated by a serial dilution of 0.16 mM sodium nitrite.

MTT assay

B16F10 cells were seeded on 96-well plates (2×10^3cells/well) and treated with DATS (10–100 μM). After 48h 25 µL of 3-(4,5-dimethyl-2-thiazolyl)-2,5-diphenyl-2 H-tetrazolium bromide (MTT) (Sigma, Milan, Italy) (5 mg/mL in saline) was added to each well. Cells were

then incubated for an additional 3 h at 37∘C. After this time interval, cells were lysed, and dark blue crystals were solubilized with a solution containing 50% N,N-dimethyl formamide and 20% SDS with an adjusted pH of 4.5. The optical density of each well was measured at 620nm with a microplate photometer reader (Multiskan FC, Thermo Scientific™, Waltham, Massachusetts, USA).

Apoptosis assay

The apoptosis of B16F10 cells was assessed by flow cytometry using annexin V‑ FITC/PI staining. Briefly, the cells were seeded into 6‑ well plates and incubated overnight. DATS 100 μM was added to the cells and incubated for 48 h. The cells were then collected, washed, and resuspended in binding buffer. The apoptotic cell death rate was examined by Annexin V‑ FITC and PI-PE double staining using the Annexin V‑ FITC apoptosis detection kit (Thermo Fisher Scientific Cat# BMS500FI/100, RRID:AB_2575598) according to the manufacturer's instructions. Following the Annexin V and PI staining, the cells were subjected to flow cytometric analysis. A minimum of 20,000 events for each sample were collected and data were analyzed using using BriCyte E6 (Mindray, P.R. China).

Statistical analysis

Data are expressed as mean ± SEM. Statistical analysis was performed with a number of n ≥ 5. Data were analysed with GrapdPad Prism 6.0 software program (GraphPad Software Inc., San Diego, CA, USA). Statistical significance between the two groups was determined by unpaired Student's t-test. A value of p-values < 0.05 was considered statistically significant. The data and statistical analysis in this study comply with the recommendations on experimental design and analysis in pharmacology (Curtis *et al.,* 2018).

Materials

DATS (LKT Laboratories) was diluted in DMSO to produce a stock solution of 10 mM for in vitro experiments. For the treatment in mice, DATS was dissolved in 0.5% carboxymethyl cellulose/0.1% DMSO in double distilled water and administered at the dose of 50mg/Kg.

Nomenclature of targets and ligands

Key protein targets and ligands in this article are hyperlinked to corresponding entries in http://www.guidetopharmacology.org, the common portal for data from the IUPHAR/BPS Guide to PHARMACOLOGY (Harding *et al.*, 2018), and are permanently archived in the Concise Guide to PHARMACOLOGY 2017/18 (Alexander *et al.*, 2017)(Alexander *et al.*, 2017).

Results

DATS inhibits tumor growth of B16F10-bearing mice by stimulating the production of H$_2$S

C57BL/6 mice were injected s.c. with 1×10^5 B16F10 melanoma cells and daily treated with DATS 50 mg/kg or vehicle, for 21 days. As shown in Figure 1A DATS-treated mice displayed a significant (P<0.001) inhibition of tumor growth of about 75% (0.232± 0.003 cm^3 mean tumor volume) as compared to the vehicle control group (0.933± 0.07 cm^3 mean tumor volume). Western blot analysis of whole tumor lysates showed a significant increase of CSE and CBS expression in melanoma samples following DATS treatment with a greater effect on CSE expression (Figure 1B-C). In addition, an enhancement of circulating H$_2$S levels were observed in the plasma of treated mice compared to untreated mice (Figure 1D), confirming that H$_2$S generation promoted the antitumor effects of DATS in this melanoma model.

DATS reduces MDSCs subsets in tumor, spleen and peripheral blood of B16F10-bearing mice

Tumor progression is strongly sustained by immunosuppressive cells like MDSCs. These cells, by inhibiting cytotoxic T cell proliferation and activation, induce failure of the antitumour immune response and lead to chemoresistance (Groth *et al.*, 2019). Thus, we hypothesized that, the anti-tumor effect displayed by DATS was related not only to its pro-apoptotic effect on B16F10 cells (Supplementary Figure 1), but also to its ability to shape the immune cell composition in melanoma-bearing mice. MDSCs have been previously identified and classified, based on the expression of the cell surface markers CD11b, Ly6C and Ly6G, in granulocytic (gr, Ly6C^{low}Ly6G^{+}C) and monocytic (mo, Ly6C^{high}Ly6G^{-}) subsets (Bronte *et al.*, 2016). In agreement with numerous previous researches, we found that melanoma growth was associated with substantial accumulation of MDSCs subsets in tumor, spleen and peripheral blood of mice. Three weeks after tumor cell injection we observed that almost the half of CD45$^{+/}$CD11b^{+} splenocytes had the phenotype of MDSCs with equally proportion among mo-MDSCs and gr-MDSCs (about 20%) (Figure 2A). However, in the blood of melanoma-bearing mice the frequency of gr-MDSCs was significantly higher (> 30%) (Figure 2B) whereas in the tumor, about 15% of tumor-infiltrating CD45$^{+/}$CD11b^{+} cells displayed mononuclear features (Ly6C^{high} Ly6G^{-}) and less than 5% were granulocytic (Ly6C^{low} Ly6G^{+}) (Figure 2C). Treatment of melanoma-bearing mice with DATS led to a significant modification of MDSCs accumulation in the different districts. In fact, in the spleen a significant (P<0.01) reduction in the percentage of both mo-MDSCs and gr-MDSCs, by 52% and 24% respectively, was observed (Figure 2A). Conversely, in the peripheral blood

only the granulocytic fraction resulted significantly restrained (Figure 2B) whereas, in tumor microenvironment, treatment with DATS significantly decreased only the proportion of the mo-MDSCs subset (Figure 2C).

DATS restores anti-tumor immune response in B16F10-bearing mice

Dendritic cells (DCs) are antigen presenting cells (APCs) that play an important role in shaping the host response to tumours (Dhodapkar *et al.*, 2008). Thus, to better elucidate the effects of DATS on immune cells composition and function in murine melanoma, we analysed the percentage of DCs, identified by the surface marker CD11c, in peripheral blood, spleen and tumour of melanoma-bearing mice. We observed a significant enrichment of DCs only in the spleen of DATS treated mice as compared to vehicle treated animals (Figure 3A). This effect was related to an increase in CD8$^+$ T cell frequencies in the spleen of DATS-treated mice as compared with untreated mice (Figure 3B). However, the number of both tumor-infiltrating and circulating CD8$^+$ T cells was not significantly modified by DATS (Figure 3C-D). Finally, we did not observe differences in the percentage of F4/80 macrophages in any compartment analyzed (data not show).

H$_2$S reduces immunosuppressive genes expression and functions in MDSCs subsets and in BM-MDSCs

It is well known that MDSCs suppress CD8$^+$ T cell function and proliferation predominantly via expression of several genes related to immunosuppressive activity such as the enzymes iNOS and ARG1 and cytokines such as IL-10, as well as, through the production of reactive nitrogen species (NOx) and reactive oxygen species (ROS) (Bronte *et al.*, 2003). Thus, in order to elucidate the mechanisms underlying DATS effect on MDSCs, we isolated and purified mo-MDSCs and gr-MDSCs from the spleen of B16F10 melanoma-bearing mice. We found that mo-MDSCs displayed significant higher ARG1 and IL-10 mRNA expression as compared to their granulocytic counterparts (Figure 4A). In fact, in mo-MDSCs ARG1 levels were almost 13-fold higher (14.6 ± 2.6 gene expression *vs* 1.9 ± 0.5 gene expression) as compared to gr-MDSCs (Figure 4A). Moreover, we found that IL-10 was expressed only in the monocytic subset. On the other hand, iNOS mRNA expression was significantly higher in gr-MDSCs as compared to mo-MDSCs (11. 8 ± 2.1 gene expression *vs* 0.09 ± 0.07 gene expression) (Figure 4A). Interestingly, in MDSCs subsets isolated from DATS-treated mice the expression of all these immunosuppressive genes resulted down-regulated as compared to MDSCs subsets isolated from untreated mice (Figure 4B). Noteworthy, following treatment with DATS, an increased expression of several genes with antioxidant activity was evident in murine melanoma tissues. DATS substantially increased the expression of both glutamate-

cysteine ligase modifier and catalytic subunits (GCLM and GCLC) and of heme oxygenase-1 (HMOX-1) whose primary function is to maintain the cellular redox balance and to reduce ROS levels (Figure 4C). Inhibition of antigen-specific $CD8^+$ T cells is the main characteristic of MDSCs function. To assess the effect of DATS on MDSCs suppression of T-cell responses, gr- and mo-MDSCs were isolated from spleens of melanoma-bearing mice and cultured with CD3/CD28 activated splenocytes. MDSCs isolated from untreated mice significantly reduced T-cell proliferation in a dose-dependent manner. We observed that, at the highest dilution rate (25%), mo-MDSCs and gr-MDSCs suppressed T-cell proliferation by 30% and 20% respectively. However, both mo- and gr-MDSCs isolated from DATS-treated mice resulted less suppressive causing a significant restoration of T-cell proliferation (Figure 4D, E).

Results obtained so far led us to hypothesize that H_2S could modify myelopoiesis within the tumor microenvironment. Thus, to investigate whether DATS might interfere on MDSCs differentiation, we induced MDSCs *ex vivo* differentiation from murine bone marrow (BM-MDSCs). BM cells were isolated from tumor-free mice and cultured for 5 days with GM-CSF and IL-4 in the presence of B16F10 conditioned medium to mimic the tumor microenvironment. The purity of the BM-MDSCs preparation was evaluated analyzing the Ly6C-Ly6G expression profile by flow cytometry. In particular, mo-MDSCs (Ly6C+, Ly6G$^-$) represented about the 30% and gr-MDSCs (Ly6C+, Ly6G^{high}) about the 15% of the total $CD11b^+$ cells (Figure 5A-B). DATS (30µM) was added on day 3rd. The concentration of DATS used was no cytotoxic for the cells (data not show). Consistent with previous observations, we found that in the presence of DATS, the proportion of MDSCs was decreased (mo-MDSCs 20.3%; gr-MDSCs 12.3%) (Figure 5A-B). In addition, we examined the effect of DATS on BM-MDSCs immunosuppressive function and we found that treatment with DATS significantly down-regulated iNOS expression in the gr-MDSCs subset whereas the ARG1 levels were not modified in mo- nor in gr-MDSCs (Figure 5C-F). The inhibition of iNOS was also confirmed by the reduction of the amounts of NO(x) in cell supernatants compared to non-treated cells (Figure 5G). Next, we asked whether the reduction of MDSCs was subsequent to their differentiation into mature myeloid cells. Thus, we evaluated the presence of $CD11c^+$ DCs in BM cells. Treatment of BM cells with DATS significantly increased the number of DCs (14.9%) that resulted almost doubled compared to non-treated cells (7.5%) (Figure 6A-B).

Discussion and Conclusion

H2S is the third gaseous signaling molecule, along with NO and carbon monoxide (CO), emerging as new actor in the pathophysiology of cancer. Recent studies indicate that H2S has both pro-cancer and anti-cancer effects. Indeed, different types of cancer utilize different H2S-associated pathways, and the final effect on cell survival/cell death mechanisms appear to be dose- and tumor cell-type-dependent (Hellmich *et al.*, 2015). We have previously demonstrated that in melanoma patient CSE expression decreases with tumor progression (Panza *et al.*, 2015) whereas others showed that overexpression of CBS enhances tumor growth and spread in colon and ovarian cancer (Bhattacharyya *et al.*, 2013; Szabo *et al.*, 2013). However, several H2S donors and H2S-releasing hybrids have been proposed as novel anti-cancer drugs. In fact relatively high concentrations of exogenous H2S could suppress cancer cells growth *via* various mechanisms, including intracellular acidification, inhibition of NF-κB activation, induction of cell death signaling and activation of caspase 3 and apoptosis (Lee *et al.*, 2011; Chattopadhyay *et al.*, 2012; Lu *et al.*, 2014; Panza *et al.*, 2015; De Cicco *et al.*, 2016; De Cicco *et al.*, 2017).

Here, we delineate a novel mechanism for the anti-cancer effect of H2S based on its ability to inhibit immunosuppressive MDSCs accumulation and functions in melanoma. Growing evidences now suggest that, even targeted agents and chemotherapies, require an endogenous immune response to induce tumor regression. Mature myeloid cells such as macrophages, DCs and granulocytes are essential for the normal function of both innate and adaptive immune systems. Unfortunately, many soluble factors present in the tumor microenvironment or released by distant sites, such as the bone marrow and spleen, alter myeloid cells differentiation and can convert them into potent immunosuppressive cells, which are known as MDSCs (Gabrilovich *et al.*, 2012). MDSCs numbers dramatically increase in tumor sites and in the spleen during tumor progression supporting tumor promotion and forming the "metastatic niche". In addition, the presence of MDSCs in the tumor microenvironment is correlated with decreased efficacy of immunotherapies making MDSCs an important target for enhancing the efficacy of cancer treatment (de Haas *et al.*, 2016). Indeed, in patients with pancreatic cancer, esophageal cancer, gastric cancer and melanoma it has been clearly demonstrated that the frequency of MDSCs in peripheral blood correlates with clinical outcomes and it has been considered an independent prognostic indicator of clinical disease progression (Jordan *et al.*, 2013). In this study, we found a positive correlation between tumor growth and MDSCs expansion in tumor, spleen and peripheral blood of melanoma-bearing mice. MDSCs were originally identified in tumor-bearing mice in two main populations: mo-MDSCs and gr-MDSCs (Bronte *et al.*, 2016). Available data strongly suggest that, in tumour-

bearing mice, gr-MDSCs represent the major subset in peripheral lymphoid organs whereas mo-MDSCs are more prominent in the tumor (Kumar *et al.*, 2016). Thus, in accordance with data present in the literature, we observed that in the spleen and in the peripheral blood of melanoma-bearing mice gr-MDSCs were largely represented, whereas the frequency of mo-MDSCs in tumor were three times higher than gr-MDSCs. Moreover, our results are in agreement with previous reports demonstrating that, in melanoma patients, the monocytic MDSCs fraction (defined as CD14$^-$ in human), plays a key role in immunosuppression and should be considered a new target for future combinatorial treatments (Jordan *et al.*, 2013). To better elucidate the mechanisms underlying the anti-tumor immune response effect promoted by H$_2$S, we treated melanoma-bearing mice with DATS, an organosulfur compounds present in garlic. Administration of DATS to melanoma bearing mice, induced up-regulation of CSE and CBS expressions, which reflected on an increase of H$_2$S plasma levels. DATS-derived H$_2$S along with the inhibition of tumor growth induced a reduction in the frequency of MDSCs in the spleen, in the blood as well as in the tumor microenvironment. Interestingly, the effect of DATS on the subtype of MDSCs was district-dependent as demonstrated by the observation that, in tumor, only mo-MDSCs subset was significantly reduced. This localized and selective effect of H$_2$S has already been observed in a model of colitis-associated cancer. In fact, administration of DATS to infected mice, induced a significant reduction of gr-MDSCs in colon, where these cells are considered to play a pivotal role in colitis development (De Cicco *et al.*, 2018). The predominant inhibitory effect displayed by DATS on mo-MDSCs was observed also in the spleen where the monocytic subset was reduced by more than 50%. Despite both mo- and gr-MDSCs were shown to efficiently suppress CD8$^+$ T-cell proliferation, mo-MDSCs have higher suppressive activity than gr-MDSCs (Movahedi *et al.*, 2008). Analogously, in our model, mo-MDSCs were found to be more potent suppressors than gr-MDSCs. In addition, we found that DATS was able to inhibit immunosuppressive activity of both subpopulations and to increase splenic CD8$^+$ T cells number, demonstrating that DATS is capable to restore T cell proliferation and function. MDSCs have been shown to suppress CD8$^+$ T cells and antitumour immune responses through multiple mechanisms. The main factors implicated in MDSCs-mediated immune suppression include ARG1, iNOS, TGFβ, IL-10, COX2, indoleamine 2,3-dioxygenase (IDO) sequestration of cysteine and many others. Mo-MDSC and gr-MDSC utilize different mechanisms for immune suppression. Indeed, the prevalence of a particular immune suppressive mechanism depends on the type of MDSCs expanded, as well as on the stage of the disease and on the site where the suppression is occurring (Movahedi *et al.*, 2008;

Gabrilovich, 2017). Interestingly, in our *in vivo* experiments DATS down-regulated iNOS, ARG-1 and IL-10 mRNA levels, which are differently expressed in spleen-derived mo- and gr-MDSCs. Furthermore, we found that treatment with DATS promoted the activation of the antioxidant pathway in melanoma-bearing mice throughout the up-regulation of GCL, the key enzyme in GSH synthesis, and HMOX-1. Moreover, by using *ex vivo*-differentiated B16F10-MDSCs, appropriately resembling *in vivo* melanoma-infiltrating MDSCs (Liechtenstein *et al.*, 2014), we demonstrated that DATS preferentially inhibited iNOS expression and NO production. This is not surprising since, recent studies, have demonstrated that NO–H_2S molecules and their enzymatic pathways may be mutually interactive and may influence each other in their production and pathophysiological functions (Kolluru *et al.*, 2013). Targeting the essential components of MDSCs-suppressive machinery resulted also in inhibition of both mo- and gr-MDSC's suppression of T-cell responses. One of the main impediments to overcome the immunosuppressive function of MDSCs is inducing their differentiation into mature myeloid cells. Notably, in melanoma-bearing mice daily treatment with DATS induced a significant increase in the number of splenic DCs, which are the APCs most likely responsible for activating T cells. Moreover, also in *in vitro* experiments we demonstrated that treatment of mouse BM immature cells with DATS resulted in reduction of MDSCs induction in favor of mature DCs differentiation. In conclusion, our results show that DATS inhibits both the expansion and the suppressive functions of MDSCs in melanoma-bearing mice with different mechanisms according to the MDSCs subset as well as their tissue of origin. In addition, DATS might reduce the presence of MDSCs by promoting their differentiation into mature APCs, preferentially DCs, suggesting a novel role for H_2S in the modulation of immune response in cancer. It is worth noting that DATS is a trisulfide compound containing the so-called sulfane sulfur in its structure. Sulfane sulfur–containing compounds are present in mammalian cells where they participate in several biological processes. They are formed during anaerobic cysteine metabolism in the reaction catalyzed mainly by CSE and 3-MST (Iciek *et al.*, 2001). However, earlier studies of Benavides et al. demonstrated non-enzymatic production of H_2S from DADS and DATS in the presence of GSH in red blood cells (Benavides *et al.*, 2007). Hence, it appears that DATS can be an exogenous source of sulfane sulfur as well as of H_2S. In this study we also found that DATS is an activator of CSE, which is involved in sulfane sulfur biosynthesis and in endogenous production of H_2S. Thus, the issue regarding the effector species being either H_2S or DATS introduced sulfane sulfur remain unsolved. Further studies are required for a better

understanding of the mechanisms underlying garlic-derived allyl sulphides therapeutic effects.

Authors Contribution

P.D.C developed the study concept, carried out in vitro and in vivo studies, statistical analysis of the results and interpretation of data for the work and drafted the manuscript. G.E. carried out in vivo experiments. V.R. carried out cytofluorimetric studies. G.R and G.T supervised over cytofluorimetric studies and interpreted data. A.I. developed the study concept, supervised over the entire study, interpreted data and provided critical revisions. All authors read and approved the final manuscript.

Declaration of transparency and scientific rigour

This Declaration acknowledges that this paper adheres to the principles for transparent reporting and scientific rigour of preclinical research as stated in the *BJP* guidelines for Design & Analysis, Immunoblotting and Immunochemistry, and Animal Experimentation, and as recommended by funding agencies, publishers and other organisations engaged with supporting research.

References

Alexander SP, Fabbro D, Kelly E, Marrion NV, Peters JA, Faccenda E, *et al.* (2017). THE CONCISE GUIDE TO PHARMACOLOGY 2017/18: Enzymes. *British journal of pharmacology* **174 Suppl 1:** S272-S359.

Benavides GA, Squadrito GL, Mills RW, Patel HD, Isbell TS, Patel RP, *et al.* (2007). Hydrogen sulfide mediates the vasoactivity of garlic. *Proceedings of the National Academy of Sciences of the United States of America* **104**(46)**:** 17977-17982.

Bhattacharyya S, Saha S, Giri K, Lanza IR, Nair KS, Jennings NB, *et al.* (2013). Cystathionine beta-synthase (CBS) contributes to advanced ovarian cancer progression and drug resistance. *PloS one* **8**(11)**:** e79167.

Bronte V, Brandau S, Chen SH, Colombo MP, Frey AB, Greten TF, *et al.* (2016). Recommendations for myeloid-derived suppressor cell nomenclature and characterization standards. *Nat Commun* **7:** 12150.

Bronte V, Serafini P, Mazzoni A, Segal DM, Zanovello P (2003). L-arginine metabolism in myeloid cells controls T-lymphocyte functions. *Trends Immunol* **24**(6)**:** 302-306.

Chattopadhyay M, Kodela R, Nath N, Barsegian A, Boring D, Kashfi K (2012). Hydrogen sulfide-releasing aspirin suppresses NF-kappaB signaling in estrogen receptor negative breast cancer cells in vitro and in vivo. *Biochemical pharmacology* **83**(6)**:** 723-732.

Condamine T, Ramachandran I, Youn JI, Gabrilovich DI (2015). Regulation of tumor metastasis by myeloid-derived suppressor cells. *Annu Rev Med* **66:** 97-110.

Curtis M. J., Alexander S., Cirino G., Docherty J. R., George C. H., Giembycz M. A., … Ahluwalia A. (2018). Experimental design and analysis and their reporting II: Updated and simplified guidance for authors and peer reviewers. British Journal of Pharmacology, 175(7), 987–993. 10.1111/bph.14153

De Cicco P, Panza E, Armogida C, Ercolano G, Taglialatela-Scafati O, Shokoohinia Y, *et al.* (2017). The Hydrogen Sulfide Releasing Molecule Acetyl Deacylasadisulfide Inhibits Metastatic Melanoma. *Front Pharmacol* **8:** 65.

De Cicco P, Panza E, Ercolano G, Armogida C, Sessa G, Pirozzi G, *et al.* (2016). ATB-346, a novel hydrogen sulfide-releasing anti-inflammatory drug, induces apoptosis of human melanoma cells and inhibits melanoma development in vivo. *Pharmacol Res* **114:** 67-73.

De Cicco P, Sanders T, Cirino G, Maloy KJ, Ianaro A (2018). Hydrogen Sulfide Reduces Myeloid-Derived Suppressor Cell-Mediated Inflammatory Response in a Model of Helicobacter hepaticus-Induced Colitis. *Frontiers in immunology* **9:** 499.

de Haas N, de Koning C, Spilgies L, de Vries IJ, Hato SV (2016). Improving cancer immunotherapy by targeting the STATe of MDSCs. *Oncoimmunology* **5**(7)**:** e1196312.

Dhodapkar MV, Dhodapkar KM, Palucka AK (2008). Interactions of tumor cells with dendritic cells: balancing immunity and tolerance. *Cell Death Differ* **15**(1)**:** 39-50.

Gabrilovich DI (2017). Myeloid-Derived Suppressor Cells. *Cancer immunology research* **5**(1)**:** 3-8.

Gabrilovich DI, Nagaraj S (2009). Myeloid-derived suppressor cells as regulators of the immune system. *Nature reviews. Immunology* **9**(3)**:** 162-174.

Gabrilovich DI, Ostrand-Rosenberg S, Bronte V (2012). Coordinated regulation of myeloid cells by tumours. *Nature reviews. Immunology* **12**(4)**:** 253-268.

Groth C, Hu X, Weber R, Fleming V, Altevogt P, Utikal J, *et al.* (2019). Immunosuppression mediated by myeloid-derived suppressor cells (MDSCs) during tumour progression. *British journal of cancer* **120**(1)**:** 16-25.

Harding SD, Sharman JL, Faccenda E, Southan C, Pawson AJ, Ireland S, *et al.* (2018). The IUPHAR/BPS Guide to PHARMACOLOGY in 2018: updates and expansion to encompass the new guide to IMMUNOPHARMACOLOGY. *Nucleic acids research* **46**(D1)**:** D1091-D1106.

Hellmich MR, Szabo C (2015). Hydrogen Sulfide and Cancer. *Handbook of experimental pharmacology* **230:** 233-241.

Iciek M, Wlodek L (2001). Biosynthesis and biological properties of compounds containing highly reactive, reduced sulfane sulfur. *Polish journal of pharmacology* **53**(3)**:** 215-225.

Jordan KR, Amaria RN, Ramirez O, Callihan EB, Gao D, Borakove M*, et al.* (2013). Myeloid-derived suppressor cells are associated with disease progression and decreased overall survival in advanced-stage melanoma patients. *Cancer Immunol Immunother* **62**(11)**:** 1711-1722.

Kerkar SP, Restifo NP (2012). Cellular constituents of immune escape within the tumor microenvironment. *Cancer research* **72**(13)**:** 3125-3130.

Kilkenny C, Browne W, Cuthill IC, Emerson M, Altman DG, Group NCRRGW (2010). Animal research: reporting in vivo experiments: the ARRIVE guidelines. *British journal of pharmacology* **160**(7)**:** 1577-1579.

Kolluru GK, Shen X, Kevil CG (2013). A tale of two gases: NO and H2S, foes or friends for life? *Redox Biol* **1:** 313-318.

Kumar V, Patel S, Tcyganov E, Gabrilovich DI (2016). The Nature of Myeloid-Derived Suppressor Cells in the Tumor Microenvironment. *Trends Immunol* **37**(3)**:** 208-220.

Lee ZW, Zhou J, Chen CS, Zhao Y, Tan CH, Li L*, et al.* (2011). The slow-releasing hydrogen sulfide donor, GYY4137, exhibits novel anti-cancer effects in vitro and in vivo. *PloS one* **6**(6)**:** e21077.

Liechtenstein T, Perez-Janices N, Gato M, Caliendo F, Kochan G, Blanco-Luquin I*, et al.* (2014). A highly efficient tumor-infiltrating MDSC differentiation system for discovery of anti-neoplastic targets, which circumvents the need for tumor establishment in mice. *Oncotarget* **5**(17)**:** 7843-7857.

Lu S, Gao Y, Huang X, Wang X (2014). GYY4137, a hydrogen sulfide (H(2)S) donor, shows potent anti-hepatocellular carcinoma activity through blocking the STAT3 pathway. *Int J Oncol* **44**(4)**:** 1259-1267.

McGrath JC, Lilley E (2015). Implementing guidelines on reporting research using animals (ARRIVE etc.): new requirements for publication in BJP. *British journal of pharmacology* **172**(13)**:** 3189-3193.

McKinney AJ, Holmen SL (2011). Animal models of melanoma: a somatic cell gene delivery mouse model allows rapid evaluation of genes implicated in human melanoma. *Chinese journal of cancer* **30**(3)**:** 153-162.

Movahedi K, Guilliams M, Van den Bossche J, Van den Bergh R, Gysemans C, Beschin A*, et al.* (2008). Identification of discrete tumor-induced myeloid-derived suppressor cell subpopulations with distinct T cell-suppressive activity. *Blood* **111**(8)**:** 4233-4244.

Panza E, De Cicco P, Armogida C, Scognamiglio G, Gigantino V, Botti G*, et al.* (2015). Role of the cystathionine gamma lyase/hydrogen sulfide pathway in human melanoma progression. *Pigment cell & melanoma research* **28**(1)**:** 61-72.

Stein A, Bailey SM (2013). Redox Biology of Hydrogen Sulfide: Implications for Physiology, Pathophysiology, and Pharmacology. *Redox Biol* **1**(1)**:** 32-39.

Szabo C, Coletta C, Chao C, Modis K, Szczesny B, Papapetropoulos A*, et al.* (2013). Tumor-derived hydrogen sulfide, produced by cystathionine-beta-synthase, stimulates bioenergetics, cell proliferation, and angiogenesis in colon cancer. *Proceedings of the National Academy of Sciences of the United States of America* **110**(30)**:** 12474-12479.

Wallace JL, Wang R (2015). Hydrogen sulfide-based therapeutics: exploiting a unique but ubiquitous gasotransmitter. *Nat Rev Drug Discov* **14**(5)**:** 329-345.

Yan Z, Banerjee R (2010). Redox remodeling as an immunoregulatory strategy. *Biochemistry* **49**(6)**:** 1059-1066.

Figure 1
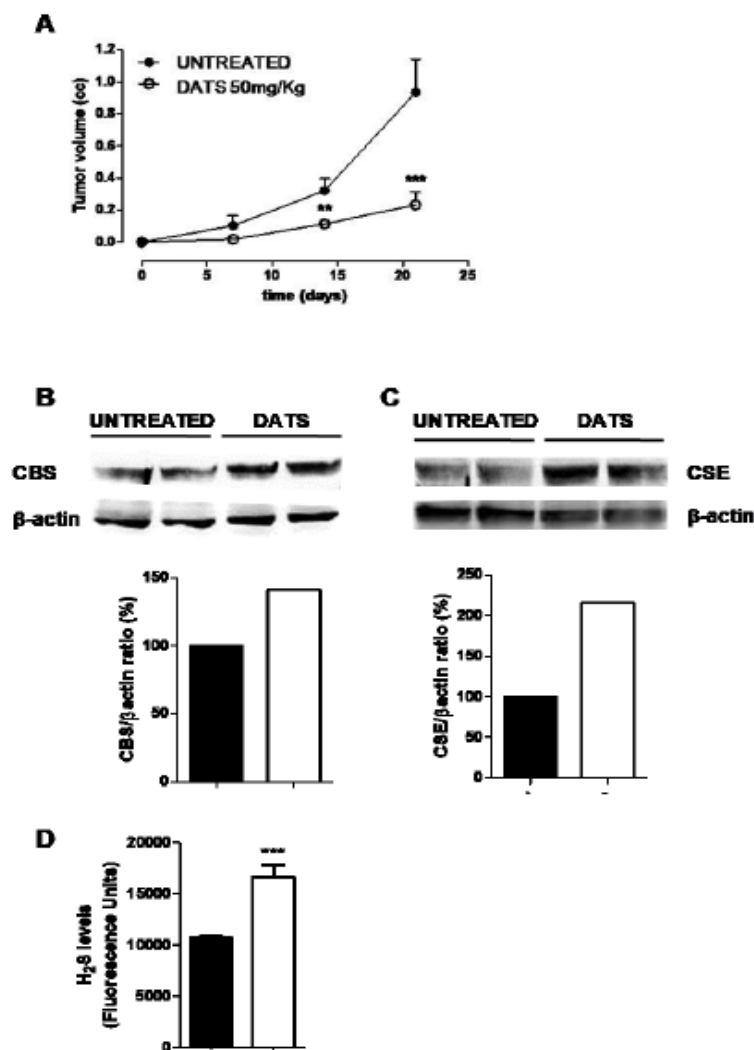
Figure 1. B16F10-melanoma bearing mice were treated daily (os) with DATS (50mg/kg) or vehicle (UNTREATED) as indicated. DATS (○) significantly reduced tumor volume compared to untreated mice (●) in a time-dependent manner. Results are presented as mean ± SEM (n = 8). **$P < 0.01$, ***$P < 0.001$ (vs UNTRATED) (A). Representative CBS and CSE expression as determined by western blot in melanoma tissues excised from melanoma-bearing mice after 21 days (n = 6). β-actin was used as loading control. Quantitative analysis of the CSE/β-actin and CBS/β-actin ratio, expressed as a percentage of the control (B-C). H₂S production in the plasma of melanoma-bearing mice was evaluated following incubation with WSP-1 (100μM) for 30 min. Data are reported as fluorescence units (n = 6). ***$P < 0.001$ (vs. untreated) (D).
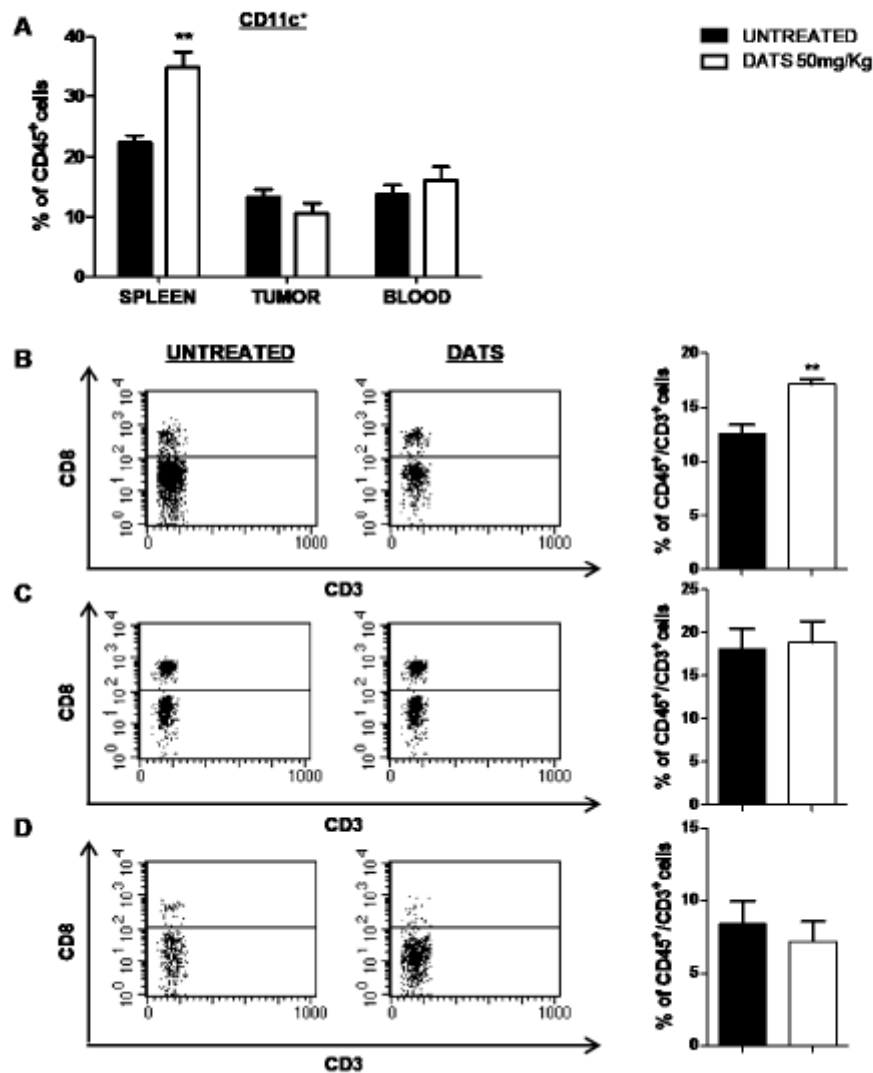
Figure 2
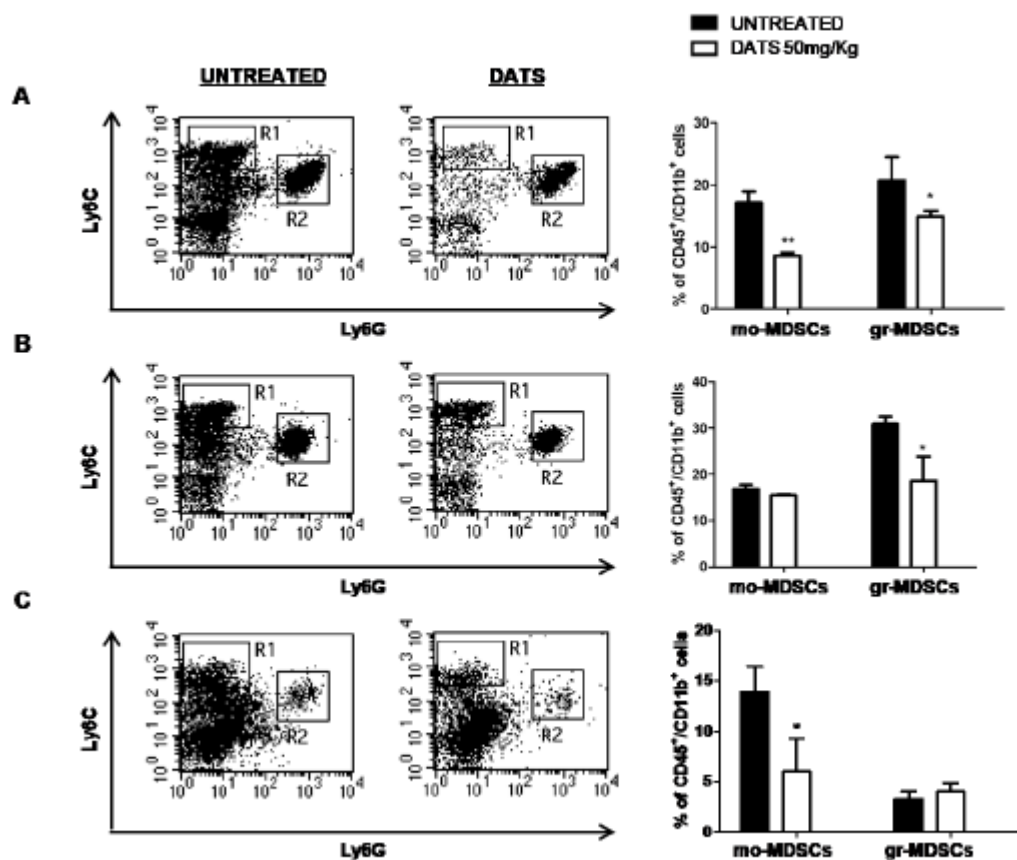
Figure 2. Flow cytometric analysis and relative quantification of mo-MDSCs (R1: Ly6C^{high} Ly6G^{-}) and gr-MDSCs (R2: Ly6C^{low} Ly6G^{+}), gated within CD45^{+}CD11b^{+} cells, in spleen (A), blood (B) and tumor (C) of melanoma-bearing mice after 21 days of treatment with DATS or vehicle (UNTREATED). Data are shown as mean ± SEM (n = 8 per group). *P<0.05, **P<0.01 (vs UNTREATED). A number of 20,000 total events was recorded.
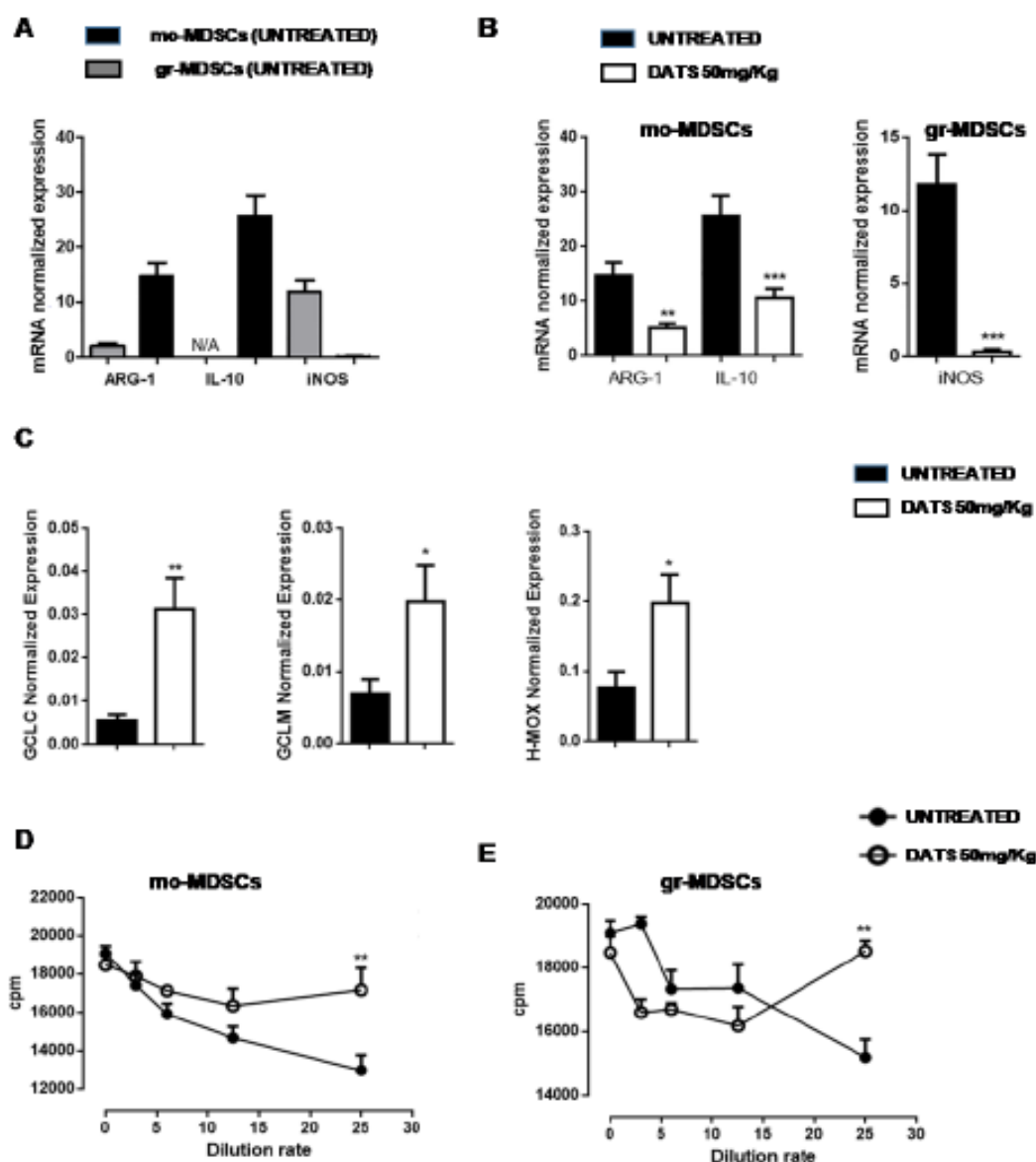
Figure 3

Figure 3. Percentage of DCs defined as $CD45^+CD11c^+$ in spleen, blood and tumor of melanoma-bearing mice after 21 days of treatment with DATS or vehicle (UNTREATED) (A). Flow cytometric analysis and relative quantification of $CD8^+$ T cells, gated within the $CD45^+CD3^+$ cells, in spleen (B), blood (C) and tumor (D) of melanoma-bearing mice after 21 days of treatment with DATS or vehicle (UNTREATED). Data are shown as mean ± SEM (n = 8 per group). **P<0.01 (vs UNTREATED). A number of 20,000 total events was recorded.
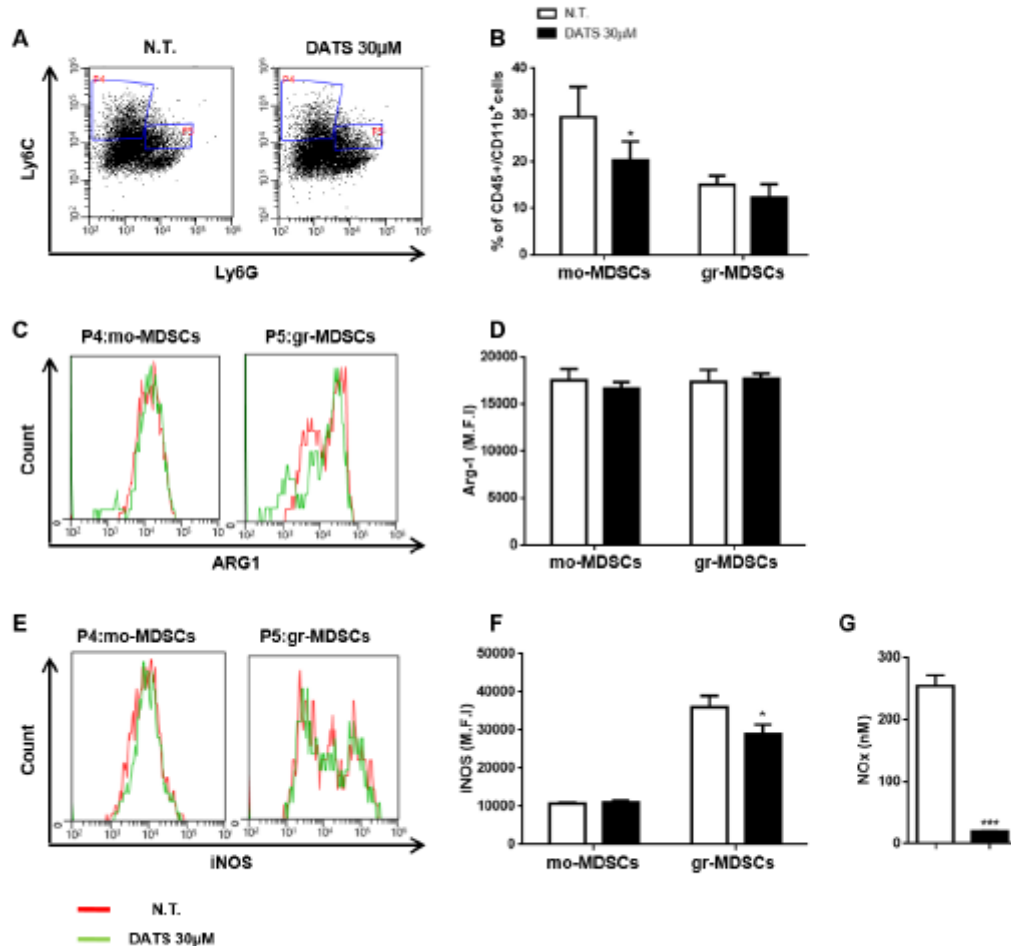
Figure 4

Figure 4. ARG1, IL-10 and iNOS mRNA levels evaluated by real-time RT-PCR in mo-MDSCs and gr-MDSCs sorted from the spleen of untreated melanoma-bearing mice after 21 days (A). ARG1, IL-10 and iNOS mRNA levels evaluated by real-time RT-PCR in mo-MDSCs and gr-MDSCs sorted from the spleen of untreated or DATS-treated melanoma-bearing mice after 21 days (B). GCLC, GCLM and HMOX mRNA levels evaluated by real-time RT-PCR in melanoma tissues excised from melanoma-bearing mice after 21 days of treatment with DATS or vehicle (UNTREATED) (C). The values were normalized to the β-actin expression. Results are presented as mean ± SEM (n=6 per group). **P < 0.01, ***P <

0.001 (vs untreated). Gr- and mo-MDSCs isolated from the spleen of melanoma-bearing mice were co-cultured at different ratio with splenocytes stimulated with coated anti-CD3 and anti-CD28 antibody, for 96h. T-cell proliferation was measured in triplicates by [^{3}H]thymidine and expressed as counts per minute (CPM). Data are shown as mean ± SEM of three separate experiments. **P<0.01, ***P < 0.001 (vs UNTREATED).

Figure 5

Figure 5. BM cells from tumor-free C57BL/6 mice were differentiate *in vitro* and cultured for 5 days with GM-CSF (10 ng/ml), IL-4 (10 ng/ml) and 30% B16F10 CM. On day 3, DATS 30μM was added at the culture. On day 5, cells were stained with CD11b, Ly6G, Ly6C, ARG1 and iNOS antibodies and analyzed by flow cytometry. Flow cyrometryc analysis (A) and relative quantification (B) of mo-MDSCs (P4: Ly6C+, Ly6G-) and gr-MDSCs (P5: Ly6C+, Ly6G^{high}), gated within CD11b$^+$ cells. Data are shown as mean ± SEM (n = 5). ARG-1 and iNOS flow cytometric analysis and relative quantification (C-F) of populations P4 and P5 as gated in (A). Data are shown as MFI ± SEM (n = 5). A number of 20,000 total events was recorded. NO(x) production was evaluated in BM-MDSCs supernatants (G). Data are shown as mean ± SEM (n = 5). *P <0.05, ***P < 0.001 (vs N.T., not treated cells).

Figure 6
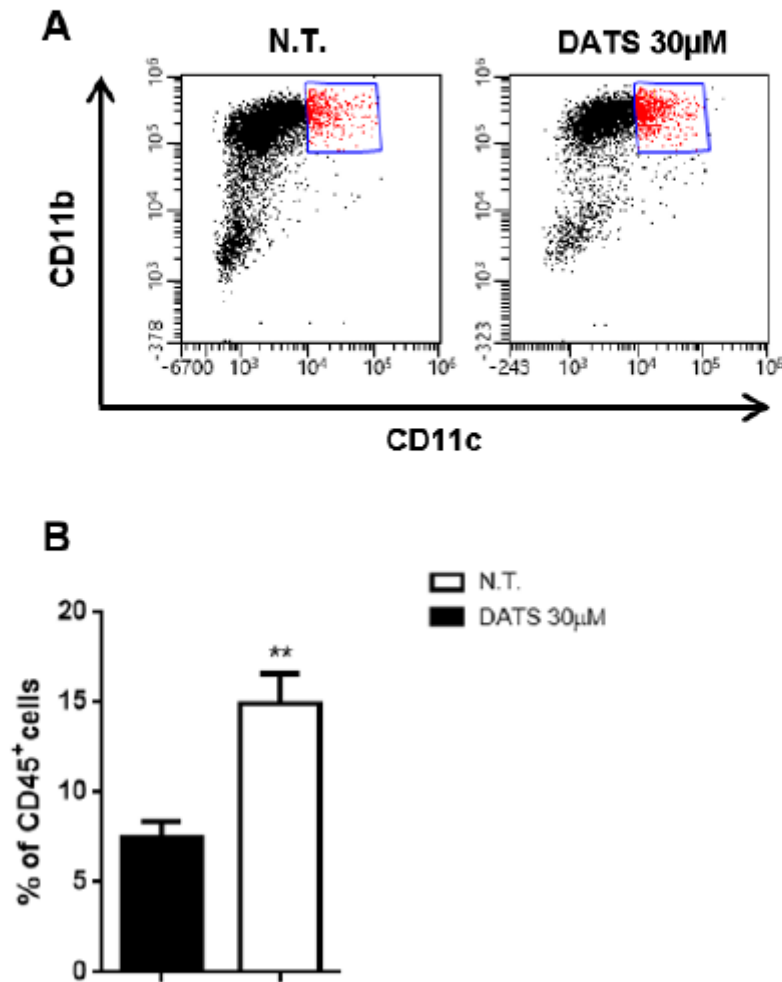
Figure 6. BM cells from tumor-free C57BL/6 mice were differentiate *in vitro* and cultured for 5 days with GM-CSF (10 ng/ml), IL-4 (10 ng/ml) and 30% B16F10 CM. On day 3, DATS 30µM was added at the culture. On day 5, cells were stained with CD45, CD11b and CD11c antibodies and analyzed by flow cytometry. Flow cyrometryc analysis (A) and relative quantification (B) of CD11b$^+$CD11c$^+$ cells, gated within CD45$^+$ cells. Data are shown as mean ± SEM (n = 5). A number of 20,000 total events was recorded. **P < 0.01 (vs N.T., not treated cells).